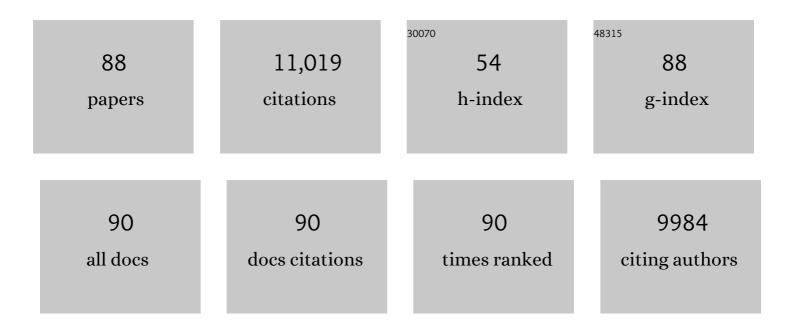
List of Publications by Year in descending order

Source: https://exaly.com/author-pdf/7912931/publications.pdf Version: 2024-02-01



WING KELHO

#	Article	IF	CITATIONS
1	Sulfur-doped g-C3N4 with enhanced photocatalytic CO2-reduction performance. Applied Catalysis B: Environmental, 2015, 176-177, 44-52.	20.2	919
2	A Hierarchical Z-Scheme CdS-WO ₃ Photocatalyst with Enhanced CO ₂ Reduction Activity. Small, 2015, 11, 5262-5271.	10.0	682
3	Fabrication and photocatalytic activity enhanced mechanism of direct Z-scheme g-C 3 N 4 /Ag 2 WO 4 photocatalyst. Applied Surface Science, 2017, 391, 175-183.	6.1	601
4	Selective photocatalytic N ₂ fixation dependent on g-C ₃ N ₄ induced by nitrogen vacancies. Journal of Materials Chemistry A, 2015, 3, 23435-23441.	10.3	495
5	Review on Metal Sulphideâ€based Zâ€scheme Photocatalysts. ChemCatChem, 2019, 11, 1394-1411.	3.7	439
6	Efficient Photocatalytic Removal of NO in Indoor Air with Hierarchical Bismuth Oxybromide Nanoplate Microspheres under Visible Light. Environmental Science & Technology, 2009, 43, 4143-4150.	10.0	426
7	Graphene-Based Photocatalysts for CO ₂ Reduction to Solar Fuel. Journal of Physical Chemistry Letters, 2015, 6, 4244-4251.	4.6	368
8	3D hierarchical graphene oxide-NiFe LDH composite with enhanced adsorption affinity to Congo red, methyl orange and Cr(VI) ions. Journal of Hazardous Materials, 2019, 369, 214-225.	12.4	329
9	Design, Fabrication, and Mechanism of Nitrogenâ€Đoped Grapheneâ€Based Photocatalyst. Advanced Materials, 2021, 33, e2003521.	21.0	324
10	Hybridization of rutile TiO2 (rTiO2) with g-C3N4 quantum dots (CN QDs): An efficient visible-light-driven Z-scheme hybridized photocatalyst. Applied Catalysis B: Environmental, 2017, 202, 611-619.	20.2	296
11	Photocatalytic H2 evolution on graphdiyne/g-C3N4 hybrid nanocomposites. Applied Catalysis B: Environmental, 2019, 255, 117770.	20.2	284
12	Copolymerization with 2,4,6-Triaminopyrimidine for the Rolling-up the Layer Structure, Tunable Electronic Properties, and Photocatalysis of g-C ₃ N ₄ . ACS Applied Materials & Interfaces, 2015, 7, 5497-5505.	8.0	264
13	Environment-Friendly Carbon Quantum Dots/ZnFe ₂ O ₄ Photocatalysts: Characterization, Biocompatibility, and Mechanisms for NO Removal. Environmental Science & Technology, 2017, 51, 2924-2933.	10.0	260
14	Fabrication of Bi2O2CO3/g-C3N4 heterojunctions for efficiently photocatalytic NO in air removal: In-situ self-sacrificial synthesis, characterizations and mechanistic study. Applied Catalysis B: Environmental, 2016, 199, 123-133.	20.2	214
15	Roles of N-Vacancies over Porous g-C ₃ N ₄ Microtubes during Photocatalytic NO <i>_x</i> Removal. ACS Applied Materials & Interfaces, 2019, 11, 10651-10662.	8.0	210
16	Efficient Visible Light Photocatalytic Removal of NO with BiOBr-Graphene Nanocomposites. Journal of Physical Chemistry C, 2011, 115, 25330-25337.	3.1	208
17	Enhancement in the photocatalytic H2 production activity of CdS NRs by Ag2S and NiS dual cocatalysts. Applied Catalysis B: Environmental, 2021, 288, 119994.	20.2	189
18	Synthesis of a Bi2O2CO3/ZnFe2O4 heterojunction with enhanced photocatalytic activity for visible light irradiation-induced NO removal. Applied Catalysis B: Environmental, 2018, 234, 70-78.	20.2	167

#	Article	IF	CITATIONS
19	High-surface area mesoporous Pt/TiO 2 hollow chains for efficient formaldehyde decomposition at ambient temperature. Journal of Hazardous Materials, 2016, 301, 522-530.	12.4	162
20	Facile synthesis of porous graphene-like carbon nitride (C6N9H3) with excellent photocatalytic activity for NO removal. Applied Catalysis B: Environmental, 2015, 174-175, 477-485.	20.2	159
21	Self doping promoted photocatalytic removal of no under visible light with bi2moo6: Indispensable role of superoxide ions. Applied Catalysis B: Environmental, 2016, 182, 316-325.	20.2	157
22	Self-assembly synthesis of boron-doped graphitic carbon nitride hollow tubes for enhanced photocatalytic NOx removal under visible light. Applied Catalysis B: Environmental, 2018, 239, 352-361.	20.2	154
23	Photocatalytic activity of Ag ₂ MO ₄ (M = Cr, Mo, W) photocatalysts. Journal of Materials Chemistry A, 2015, 3, 20153-20166.	10.3	152
24	Review on nickel-based adsorption materials for Congo red. Journal of Hazardous Materials, 2021, 403, 123559.	12.4	148
25	Hierarchical NiO–SiO2 composite hollow microspheres with enhanced adsorption affinity towards Congo red in water. Journal of Colloid and Interface Science, 2016, 466, 238-246.	9.4	133
26	Visible-Light-Active Plasmonic Ag–SrTiO ₃ Nanocomposites for the Degradation of NO in Air with High Selectivity. ACS Applied Materials & Interfaces, 2016, 8, 4165-4174.	8.0	132
27	Enhanced visible-light-driven photocatalytic removal of NO: Effect on layer distortion on g-C3N4 by H2 heating. Applied Catalysis B: Environmental, 2015, 179, 106-112.	20.2	131
28	Perovskite LaFeO3-SrTiO3 composite for synergistically enhanced NO removal under visible light excitation. Applied Catalysis B: Environmental, 2017, 204, 346-357.	20.2	127
29	g ₃ N ₄ â€Based 2D/2D Composite Heterojunction Photocatalyst. Small Structures, 2021, 2, 2100086.	12.0	127
30	Biocompatible FeOOH-Carbon quantum dots nanocomposites for gaseous NO removal under visible light: Improved charge separation and High selectivity. Journal of Hazardous Materials, 2018, 354, 54-62.	12.4	126
31	Protonated g-C3N4/Ti3+ self-doped TiO2 nanocomposite films: Room-temperature preparation, hydrophilicity, and application for photocatalytic NO removal. Applied Catalysis B: Environmental, 2019, 240, 122-131.	20.2	122
32	Improved Oxygen Activation over a Carbon/Co ₃ O ₄ Nanocomposite for Efficient Catalytic Oxidation of Formaldehyde at Room Temperature. Environmental Science & Technology, 2021, 55, 4054-4063.	10.0	97
33	Photocatalytic selective oxidation of phenol to produce dihydroxybenzenes in a TiO 2 /UV system: Hydroxyl radical versus hole. Applied Catalysis B: Environmental, 2016, 199, 405-411.	20.2	95
34	Photocatalytic NO removal on BiOI surface: The change from nonselective oxidation to selective oxidation. Applied Catalysis B: Environmental, 2015, 168-169, 490-496.	20.2	88
35	Enhanced solar-to-chemical energy conversion of graphitic carbon nitride by two-dimensional cocatalysts. EnergyChem, 2021, 3, 100051.	19.1	87
36	Enhanced catalytic activity of hierarchically macro-/mesoporous Pt/TiO ₂ toward room-temperature decomposition of formaldehyde. Catalysis Science and Technology, 2015, 5, 2366-2377.	4.1	86

#	Article	IF	CITATIONS
37	TiO2/In2S3 S-scheme photocatalyst with enhanced H2O2-production activity. Nano Research, 2023, 16, 4506-4514.	10.4	85
38	Nearâ€Infraredâ€Responsive Photocatalysts. Small Methods, 2021, 5, e2001042.	8.6	84
39	Photocatalytic CO ₂ reduction of C/ZnO nanofibers enhanced by an Ni-NiS cocatalyst. Nanoscale, 2020, 12, 7206-7213.	5.6	80
40	Graphene-induced formation of visible-light-responsive SnO2-Zn2SnO4 Z-scheme photocatalyst with surface vacancy for the enhanced photoreactivity towards NO and acetone oxidation. Chemical Engineering Journal, 2018, 336, 200-210.	12.7	79
41	Hierarchical Pt/NiO Hollow Microspheres with Enhanced Catalytic Performance. ChemNanoMat, 2015, 1, 58-67.	2.8	78
42	Tuning the strength of built-in electric field in 2D/2D g-C3N4/SnS2 and g-C3N4/ZrS2 S-scheme heterojunctions by nonmetal doping. Journal of Materiomics, 2021, 7, 988-997.	5.7	77
43	Photocatalytic removal of NO and HCHO over nanocrystalline Zn2SnO4 microcubes for indoor air purification. Journal of Hazardous Materials, 2010, 179, 141-150.	12.4	75
44	Hierarchically porous NiO–Al ₂ O ₃ nanocomposite with enhanced Congo red adsorption in water. RSC Advances, 2016, 6, 10272-10279.	3.6	72
45	Controllable Synthesis of Core–Shell Bi@Amorphous Bi ₂ O ₃ Nanospheres with Tunable Optical and Photocatalytic Activity for NO Removal. Industrial & Engineering Chemistry Research, 2017, 56, 10251-10258.	3.7	66
46	In situ Fabrication of α-Bi2O3/(BiO)2CO3 Nanoplate Heterojunctions with Tunable Optical Property and Photocatalytic Activity. Scientific Reports, 2016, 6, 23435.	3.3	65
47	Room-temperature formaldehyde catalytic decomposition. Environmental Science: Nano, 2020, 7, 3655-3709.	4.3	64
48	Facile fabrication of porous Cr-doped SrTiO ₃ nanotubes by electrospinning and their enhanced visible-light-driven photocatalytic properties. Journal of Materials Chemistry A, 2015, 3, 3935-3943.	10.3	62
49	Hierarchical porous Al2O3@ZnO core-shell microfibres with excellent adsorption affinity for Congo red molecule. Applied Surface Science, 2019, 473, 251-260.	6.1	61
50	Constructing Z-scheme SnO ₂ /N-doped carbon quantum dots/ZnSn(OH) ₆ nanohybrids with high redox ability for NO <i>x</i> removal under VIS-NIR light. Journal of Materials Chemistry A, 2019, 7, 15782-15793.	10.3	60
51	Highly Selective Photocatalytic CO ₂ Methanation with Water Vapor on Singleâ€Atom Platinumâ€Decorated Defective Carbon Nitride. Angewandte Chemie - International Edition, 2022, 61, .	13.8	60
52	Phosphorus flame retardants and Bisphenol A in indoor dust and PM2.5 in kindergartens and primary schools in Hong Kong. Environmental Pollution, 2018, 235, 365-371.	7.5	59
53	Effects of H2O2 generation over visible light-responsive Bi/Bi2O2â^'CO3 nanosheets on their photocatalytic NO removal performance. Chemical Engineering Journal, 2019, 363, 374-382.	12.7	56
54	<i>In situ</i> g-C ₃ N ₄ self-sacrificial synthesis of a g-C ₃ N ₄ /LaCO ₃ OH heterostructure with strong interfacial charge transfer and separation for photocatalytic NO removal. Journal of Materials Chemistry A, 2018, 6, 972-981.	10.3	54

#	Article	IF	CITATIONS
55	Enhanced photocatalytic removal of NO over titania/hydroxyapatite (TiO ₂ /HAp) composites with improved adsorption and charge mobility ability. RSC Advances, 2017, 7, 24683-24689.	3.6	52
56	Construction of the 1D Covalent Organic Framework/2D g-C ₃ N ₄ Heterojunction with High Apparent Quantum Efficiency at 500 nm. ACS Applied Materials & Interfaces, 2020, 12, 51555-51562.	8.0	50
57	Synthesis of SrFexTi1-xO3-l̂´ nanocubes with tunable oxygen vacancies for selective and efficient photocatalytic NO oxidation. Applied Catalysis B: Environmental, 2018, 239, 1-9.	20.2	46
58	Graphdiyne: A Brilliant Hole Accumulator for Stable and Efficient Planar Perovskite Solar Cells. Small, 2020, 16, e1907290.	10.0	45
59	Lowâ€Temperatureâ€Processed Zr/F Coâ€Doped SnO ₂ Electron Transport Layer for Highâ€Efficiency Planar Perovskite Solar Cells. Solar Rrl, 2020, 4, 2000090.	5.8	42
60	Simultaneous excitation of PdCl2 hybrid mesoporous g-C3N4 molecular/solid-state photocatalysts for enhancing the visible-light-induced oxidative removal of nitrogen oxides. Applied Catalysis B: Environmental, 2016, 184, 174-181.	20.2	39
61	Active Complexes on Engineered Crystal Facets of MnO _x –CeO ₂ and Scale-Up Demonstration on an Air Cleaner for Indoor Formaldehyde Removal. Environmental Science & Technology, 2019, 53, 10906-10916.	10.0	36
62	Grapheneâ€Based Materials in Planar Perovskite Solar Cells. Solar Rrl, 2020, 4, 2000502.	5.8	36
63	Synthesis of mesoporous polymeric carbon nitride exhibiting enhanced and durable visible light photocatalytic performance. Science Bulletin, 2014, 59, 688-698.	1.7	33
64	Synthesis and characterization of Bi-BiPO4 nanocomposites as plasmonic photocatalysts for oxidative NO removal. Applied Surface Science, 2020, 513, 145775.	6.1	32
65	Graphdiyne-based photocatalysts for solar fuel production. Green Chemistry, 2022, 24, 5739-5754.	9.0	30
66	Metal–Organic Frameworks for NO <i>_x</i> Adsorption and Their Applications in Separation, Sensing, Catalysis, and Biology. Small, 2022, 18, e2105484.	10.0	29
67	Novel N/Carbon Quantum Dot Modified MIL-125(Ti) Composite for Enhanced Visible-Light Photocatalytic Removal of NO. Industrial & Engineering Chemistry Research, 2020, 59, 6470-6478.	3.7	26
68	Controllable synthesis of phosphate-modified BiPO ₄ nanorods with high photocatalytic activity: surface hydroxyl groups concentrations effects. RSC Advances, 2015, 5, 99712-99721.	3.6	24
69	Photocatalytic Air Purification Using Functional Polymeric Carbon Nitrides. Advanced Science, 2021, 8, e2102376.	11.2	24
70	g ₃ N ₄ /TiO ₂ Composite Film in the Fabrication of a Photocatalytic Airâ€Purifying Pavements. Solar Rrl, 2020, 4, 2000170.	5.8	23
71	The role and synergistic effect of the light irradiation and H2O2 in photocatalytic inactivation of Escherichia coli. Journal of Photochemistry and Photobiology B: Biology, 2015, 149, 164-171.	3.8	22
72	Mechanism of NO Photocatalytic Oxidation on g-C3N4 Was Changed by Pd-QDs Modification. Molecules, 2016, 21, 36.	3.8	22

WING KEI HO

#	Article	lF	CITATIONS
73	Exploring the photocatalytic conversion mechanism of gaseous formaldehyde degradation on TiO2–-OV surface. Journal of Hazardous Materials, 2022, 424, 127217.	12.4	22
74	Unraveling the mechanisms of room-temperature catalytic degradation of indoor formaldehyde and its biocompatibility on colloidal TiO ₂ -supported MnO _x –CeO ₂ . Environmental Science: Nano, 2018, 5, 1130-1139.	4.3	21
75	Ultra violet filters in the urine of preschool children and drinking water. Environment International, 2019, 133, 105246.	10.0	20
76	Reasonable design of Cu2MoS4 heterophase junction for highly efficient photocatalysis. Journal of Alloys and Compounds, 2020, 826, 154076.	5.5	18
77	Efficient photocatalytic degradation of NO by ceramic foam air filters coated with mesoporous TiO2 thin films. Chinese Journal of Catalysis, 2015, 36, 2109-2118.	14.0	16
78	A Review of Co3O4-based Catalysts for Formaldehyde Oxidation at Low Temperature: Effect Parameters and Reaction Mechanism. Aerosol Science and Engineering, 2020, 4, 147-168.	1.9	16
79	Organophosphate flame retardants and bisphenol A in children's urine in Hong Kong: has the burden been underestimated?. Ecotoxicology and Environmental Safety, 2019, 183, 109502.	6.0	15
80	The photocatalytic NO-removal activity of g-C ₃ N ₄ significantly enhanced by the synergistic effect of Pd ⁰ nanoparticles and N vacancies. Environmental Science: Nano, 2022, 9, 742-750.	4.3	15
81	Construction and Activity of an Allâ€Organic Heterojunction Photocatalyst Based on Melem and Pyromellitic Dianhydride. ChemSusChem, 2022, 15, e202200477.	6.8	15
82	Highly efficient photocatalytic degradation for antibiotics and mechanism insight for Bi2S3/g-C3N4 with fast interfacial charges transfer and excellent stability. Arabian Journal of Chemistry, 2022, 15, 103689.	4.9	12
83	Oxygen vacancy-dependent photocatalytic activity of well-defined Bi ₂ Sn ₂ O _{7â^'x} hollow nanocubes for NO _x removal. Environmental Science: Nano, 2021, 8, 1927-1933.	4.3	11
84	Photocatalytic reactive oxygen species generation activity of TiO ₂ improved by the modification of persistent free radicals. Environmental Science: Nano, 2021, 8, 3846-3854.	4.3	11
85	In Situ Intermediates Determination and Cytotoxicological Assessment in Catalytic Oxidation of Formaldehyde: Implications for Catalyst Design and Selectivity Enhancement under Ambient Conditions. Environmental Science & Technology, 2019, 53, 5230-5240.	10.0	10
86	Efficient Visible Light Photocatalytic Oxidation of NO on F- and N-Codoped Spherical <mml:math xmlns:mml="http://www.w3.org/1998/Math/MathML" id="M1"><mml:mrow><mml:msub><mml:mrow><mml:mtext>TiO</mml:mtext></mml:mrow><mml:mtext mathvariant="bold">2</mml:mtext </mml:msub><mml:mrow></mml:mrow>Synthesized via Ultrasonic</mml:mrow></mml:math 	2.7	8
87	Spray Pyrolysis. Journal of Nanomaterials, 2012, 2012, 1-9. Construction and Activity of an Allâ€Organic Heterojunction Photocatalyst Based on Melem and Pyromellitic Dianhydride. ChemSusChem, 2022, 15, .	6.8	2
88	Unraveling the Reaction Mechanism of HCHO Catalytic Oxidation on Pristine Co3O4 (110) Surface: A Theoretical Study. Catalysts, 2022, 12, 560.	3.5	1